Desalination and Water Treatment
www.deswater.com
doi: 10.1080/19443994.2015.1080193

57 (2016) 16466–16472
July

Taylor & Francis
Taylor & Francis Group

Removal of ethylenediaminetetraacetic acid and its cobalt complex by layered double hydroxide/titanium dioxide from aqueous solution

Reda R. Sheha[a], Ahmed H. Harb[a,*], Ibrahim El-T. El-sayed[b], Hanan H. Someda[a]

[a]*Nuclear Chemistry Department, Hot Laboratories Center, Atomic Energy Authority, Cairo, Egypt, email: rsheha68@yahoo.com (R.R. Sheha), Tel. +2 01159724053; emails: harb_chem@yahoo.com, harbchem22@gmail.com (A.H. Harb), hanan_someda@yahoo.com (H.H. Someda)*
[b]*Faculty of Science, Chemistry Department, Menoufia University, El menoufia, Egypt, email: ibrahimtantawy@yahoo.co.uk*

Received 23 March 2015; Accepted 28 July 2015

ABSTRACT

TiO_2–LDH photocatalysts as mechanical mixture (MCPC) and core-shell (CSPC) were successfully synthesized and characterized by XRD, TEM, and EDX techniques. The band gaps were determined by UV–vis diffuse reflectance. The photocatalytic efficiency of the catalysts for removal of ethylenediaminetetraacetic acid (EDTA) and its cobalt complexes (Co(II)-EDTA) was evaluated under ultraviolet (UV) irradiation. Results showed that the employed catalysts not only has higher removal efficiency for both EDTA and Co(II)-EDTA than TiO_2, but also easily separated from the aqueous phase. Removal percentages of about 83 and 88% (for EDTA) and 71 and 81% (for Co(II)-EDTA) are achieved by MMPC and CSPC, respectively.

Keywords: Mechanical mixture; Titanium; Core shell; Photocatalytic degradation; EDTA

1. Introduction

From the view point of environmental issue, the remediation of persistent organic pollutants has a great interest and importance [1,2]. Ethylenediaminetetraacetic acid (EDTA) is widely used in industrial, pharmaceutical, and agricultural applications. Wastewater containing EDTA becomes an environmental concern [3,4]. This is due to the possibility of toxic heavy metal mobilization, extended biological availability to aquatic life, and the subsequent risks these metals pose to groundwater and drinking water [3–5].

Unlike the conventional treatment methods (biodegradation, adsorption, and chemical treatment), advanced oxidation processes especially titanium-based photocatalysis technology offered a powerful oxidation technique for the treatment of persistent organic pollutants by mineralization into CO_2 and water [6–8].

Titanium dioxide (TiO_2) is the most widely investigated photocatalyst. This is because it has high photoactivity and high chemical and thermal stability as well as low cost and toxicity. However, there is a rapid recombination between photo-generated highly excited state (electron and holes), agglomeration, difficulty of separation, and high band gap (3.2 eV) [9–12]. Such drawbacks attract researchers to think about a strategy that can overcome these defects.

Layered double hydroxides (LDHs)/titanium semiconductors have great progress in photocatalysis [8,13,14]. LDHs are a class of promising hydrotalcite like compounds or anionic clays, of general formula $[M^{II}_{1-X}\ M^{III}_{X}\ (OH)_2]^{X+}[A^{n-}_{X/n}\cdot yH_2O]^{X-}$, where M(II) and

---

*Corresponding author.

M(III) are divalent and trivalent metal cations, respectively, A^{n-} represents interlayer anions for charge neutrality, and X is the molar ratio which has values usually ranging from 0.20 to 0.33. The hydroxide layers order is similar to that of brucite ($Mg(OH)_2$), where each Mg^{2+}cation is octahedrally surrounded by six OH^- anions and all the octahedral structures share their edges to form infinite sheets. In the LDHs, the M^{II}/M^{III} isomorphous substitution in octahedral sites of the hydroxide sheets produces a net positive charge, which is neutralized by anions accommodated between brucite layers and water molecules may occupy the remaining space of the interlayer region [15–17].

Recently, LDHs have a great attention in wastewater remediation due to its properties like unique layered structure, high anion exchange capacity, simplicity of synthesis, low costs, and recyclability [14,15,18–21].

LDH is found to enhance the probability of having mixed oxides composites because their metal might produce a defect energy level in between valence and conduction band [6,17,20]. We have been working to integrate the advantages of both titanium oxide and LDHs.

Therefore, the present work aims to synthesize two TiO_2–LDH composites, mechanical mixture photocatalyst (MMPC) and core-shell photocatalyst (CSPC), and evaluate their performance as photocatalysts for the removal of EDTA and Co(II)-EDTA complexes from aqueous solutions.

2. Materials and methods

2.1. Materials

All chemicals and reagents used in the present work were of analytical grade and used without further purification. Magnesium nitrate ($Mg(NO_3)_2{\cdot}6H_2O$) and TiO_2 were purchased from Sigma–Aldrich, while aluminum nitrate ($Al(NO_3){\cdot}9H_2O$) was purchased from Fluka. Bi-distilled water (BDW) was used throughout the experimental work.

2.2. Preparation of LDH–TiO_2 composites

2.2.1. The mechanical mixture photocatalyst

Mg/Al LDH with a molar ratio of 2:1 was prepared by co-precipitation method via slow mixing of 100 ml of 0.6 M Mg(II) and 100 ml of 0.3 M Al(III). The pH was maintained in the range 8–10 using 2 M NaOH solution while stirring under an inert atmosphere. The obtained suspension was aged at 60˚C for 24 h. The formed LDH particles were separated, washed several times with BDW, and finally dried at 90˚C till constant weight was obtained. The MMPC was prepared by mixing TiO_2 and Mg/Al LDH.

2.2.2. The core-shell photocatalyst

CSPC was prepared by simultaneous addition of 0.6 M Mg(II) and 0.3 M Al(III) solutions (100 ml of each) to 100 ml TiO_2 suspension under stirring in an inert atmosphere. The produced CSPC particles were aged at 60˚C for 24 h, then separated, washed several times with BDW, and finally dried at 90˚C till constant weight was obtained.

2.3. Photocatalytic experiments

The photocatalytic activity of the prepared materials was evaluated by the degradation of EDTA and Co-EDTA using UV lamb (254 nm, Japan) placed 5 cm above the solution. A fixed amount of the photocatalyst was added to 100 ml of either EDTA (1,000 mg/L) or Co(II)-EDTA (1,000 mg/L of each) at pH 3.5 in a Pyrex batch photoreactor under airflow.

Prior to irradiation, the suspensions were stirred for 30 min in the dark under airflow to ensure the adsorption–desorption equilibrium on the photocatalyst surface [17,22–24]. At certain time intervals, 4 ml solution was sampled and filtered through 0.45-μm Whatman membrane filter. Then, the filtrates were analyzed using UV–vis double beam PC scanning spectrophotometer (UV-2950 LABOMED, Inc. USA).

2.4. Characterization

X-ray diffraction of the employed photocatalysts was carried out by PANalytical X'Pert PRO Diffractometer using a Cu-target with Ni-filtered radiation ($\lambda = 1.542$ Å). High-resolution transmission electron microscopy (HRTEM) picture of the external surface of the catalysts was performed using a JEOL transmission electron microscope (TEM-2100) operating at an accelerating voltage of 200 kV and coupled with energy dispersive X-ray (EDX) spectrometer. UV–vis diffuse reflectance (UV–vis-DR) spectra were obtained at room temperature on a Nicolet Evolution 500 UV–vis Spectrometer with a diffuse reflectance accessory using KBr standard white as reflectance.

3. Results and discussion

3.1. Structural characterization

Fig. 1 shows that the XRD pattern of LDH, anatase, and CSPC display well crystalline materials. The

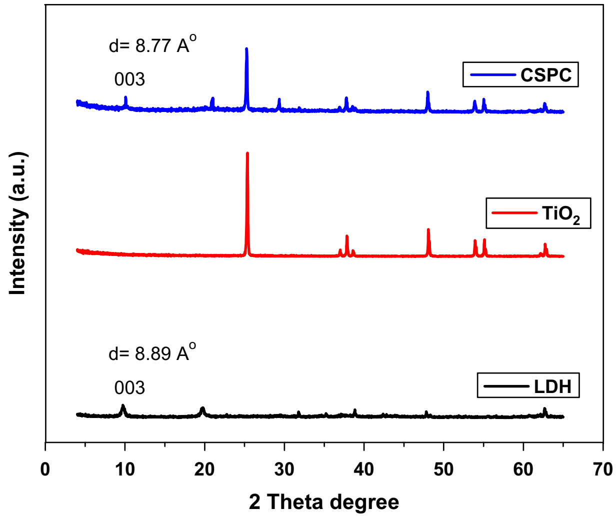

Fig. 1. XRD patterns of LDH, TiO_2, and CSPC.

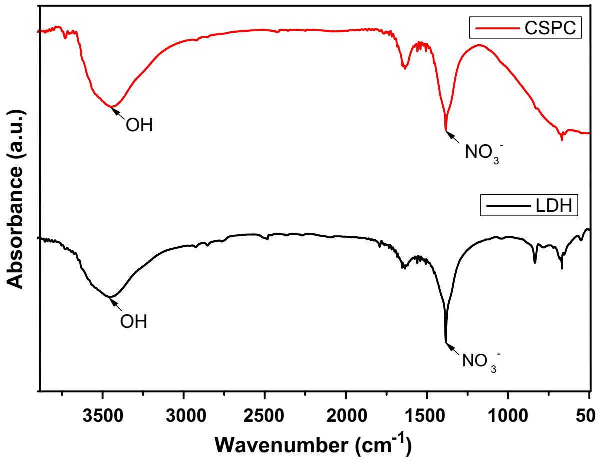

Fig. 2. FTIR spectra of MMPC and CSPC.

characteristic, symmetric, and sharp peaks (0 0 3) might be due to strong reflection of the basal planes. The (0 0 3) reflection is typical of hydrotalcite-type materials and its intensity is related to the crystallinity degree of the material [24–26]. On the other hand, the lamellar distance of the crystalline plane (0 0 3) in the XRD patterns allows the calculation of lamellar distance between layers (d-spacing). D-spacing of MMPC and CSPC are 8.89 and 8.77 Å, respectively. The CSPC structure shows both peaks of anatase and identified peaks of LDH.

FTIR spectra of the synthesized materials are shown in Fig. 2. The spectra show a broad and intensive band between 3,300 and 3,600 cm^{-1}, which might be due to the stretching vibration of the OH group of interlamellar water molecules and in brucite-like layer. The strong peak at 1,375 cm^{-1} might be attributed to stretching vibration of NO_3^- interlayer anions. The two vibration bands at 824 and 740 cm^{-1} are attributed to the stretching mode of NO_3^- [8,15]. At 3,700 cm^{-1}, a new peak appears in CSPC structure and might be due to the combination of titania and LDH. The bending mode of the OH group of water molecules appears at 1,640 cm^{-1} [16,18].

3.2. *Transmitting electron microscopy and EDX spectrum*

The transmitting electron microscopy (TEM) micrographs of the prepared materials are shown in Fig. 3.

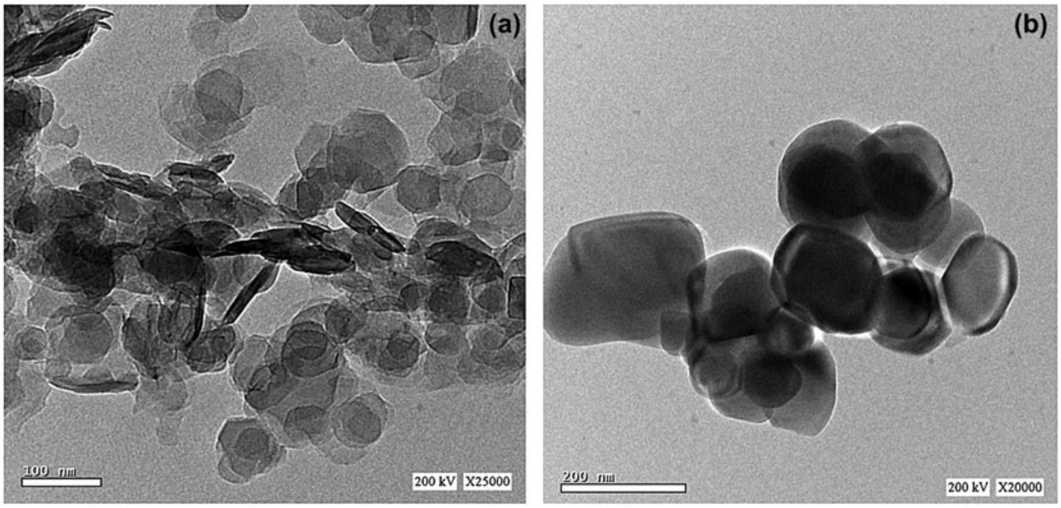

Fig. 3. TEM micrographs of (a) LDH and (b) CSPC.

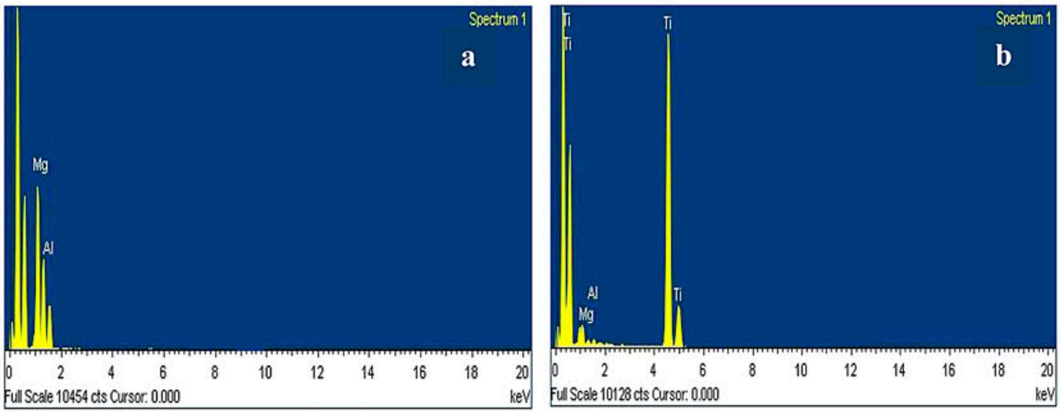

Fig. 4. EDX analysis of (a) LDH and (b) CSPC.

Fig. 3(a) shows the octahedral layer of hydrotalcite, while Fig. 3(b) of CSPC shows that the TiO_2 particles were covered by LDH. The picture reveals a dark centered core of TiO_2 covered by a homogenous pale shell of LDH [27]. The EDX patterns of the synthesized materials are illustrated in Fig. 4. The EDX plot of LDH shows peaks indicative of the presence of Mg and Al elements Fig. 4(a). It is noted that the peaks corresponding to Mg element exhibit intensity greater than that of Al. The presence of Ti^{4+} cation in the CSPC photocatalysts is confirmed through obvious EDX peaks Fig. 4(b) and titanium shows high content compared with that of Mg and Al.

3.3. Band gaps

The light absorption by the material and the migration of the light-induced electrons and holes are the most key factors controlling a photocatalytic reaction, which is relevant to the electronic structure characteristics of the material. The UV–vis absorption spectra of the catalysts are shown in Fig. 5. The absorption of CSPC is lower than that of MMPC which may be due to the lower band gap of CSPC as compared to that of MMPC. As a crystalline semiconductor, the optical absorption near the band edge follows the formula $\alpha h\upsilon = A\,(h\upsilon - Eg)^{n/2}$, where α is the absorption coefficient, υ is the light frequency, Eg is the band gap, A is a constant, and n is a constant that depends on the type of the optical transition in the semiconductor. The constant n has a value of 1 (for direct transition) or a value of 4 (for indirect transition) [7].

The band gap of the CSPC and MMPC can be obtained by plotting $(\alpha h\upsilon)^2$ vs. $h\upsilon$ as shown in Fig. 5, which illustrates that the band gaps of MMPC and CSPC are 3.4 and 2.88 eV, respectively, confirming the lower band gap of CSPC as compared to that of MMPC.

3.4. The removal efficiency

Fig. 6(a) shows the removal of EDTA by MMPC, CSPC, and TiO_2 from aqueous solution. From this figure, the removal efficiency of EDTA by MMPC and CSPC is sharply increased in the first 30 min. Further increase in the contact time, under UV irradiation, had no effect on EDTA removal by CSPC. While for MMPC, an improvement in EDTA removal was observed and a maximum removal of 83.6% is achieved at 270 min. On the other hand, insignificant removal was obtained by TiO_2 at 30 min, which indicates that this material had no affinity for EDTA species under our experimental conditions.

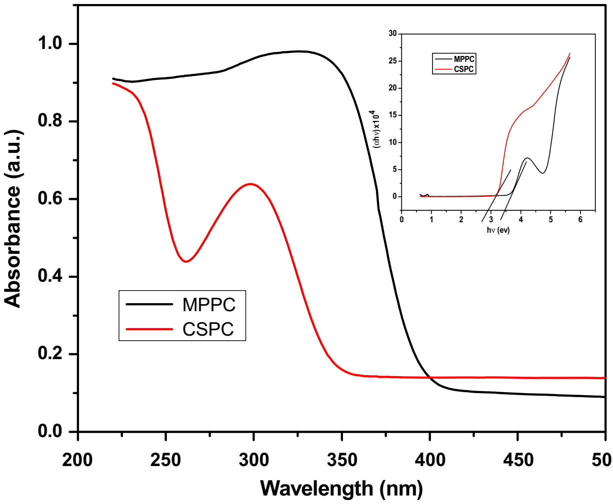

Fig. 5. UV–vis spectra of MMPC and CSPC and plotting of $(\alpha h\upsilon)^2$ vs. $h\upsilon$ of MMPC and CSPC.

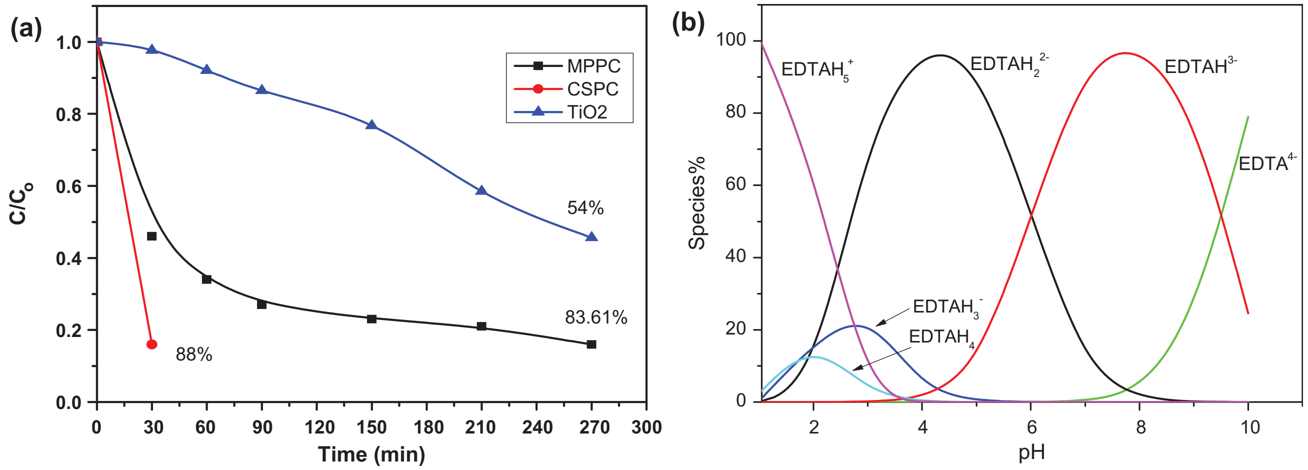

Fig. 6. Photocatalytic degradation of 1,000 mg/L EDTA using CSPC, MMPC, and TiO_2 (a) and its aqueous speciation at different pH values (b).

In order to well interpret the data obtained in Fig. 6(a), the speciation of EDTA as a function of pH, calculated by the PHREEQ software, is shown in Fig. 6(b). From this figure, it can be seen that EDTA presents in the aqueous solution as $EDTAH_3^-$ and $EDTAH_2^{2-}$ in the pH range 3.5–4. The point of zero charge (pzc) of LDH was determined experimentally and found to be around 7.5 (Figure not shown). This indicates that the surface of LDH at pH < pzc is positively charged [28]. Therefore, the removals obtained for EDTA before 30 min using MMPC and CSPC is due to adsorption rather than degradation. Based on this observation, the removals obtained for EDTA (55% for MMPC and 88% for CSPC, Fig. 6(a) can be attributed to the electrostatic attraction between EDTA anions and the positively charged hydroxide layer in LDH. The removals obtained by MMPC after 30 min may be due to synchronization between adsorption and degradation. On the contrary, the removal observed for EDTA by TiO_2 Fig. 6(a) is mainly due to photodegradation.

As shown by Fig. 7(a), the removal of Co-EDTA increases with time and a maximum removal of 71 and 81% are attained at 270 min by MMPC and CSPC,

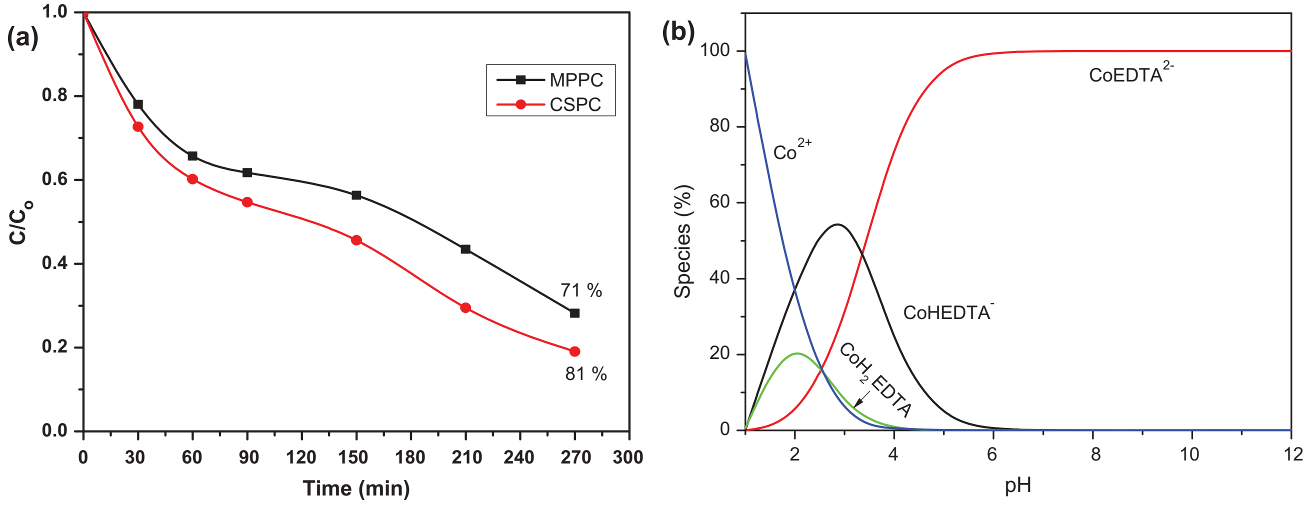

Fig. 7. Photocatalytic degradation of Co-EDTA complexes (1,000 mg/L of each) onto CSPC and MMPC (a) and its aqueous speciation at different pH values (b).

respectively. In presence of cobalt, EDTA presents in the pH range 3–4 as Co HEDTA$^-$, EDTAH$_3^-$ and EDTAH$_2^{2-}$ Fig. 7(b). This indicates that EDTA presents predominately as anionic complexes. Therefore, the removal achieved before 30 min by the employed materials Fig. 6(a) is attributed to electrostatic attraction between the negatively charged Co(II)-EDTA complexes and the positively charged LDH particles. Regarding the data obtained at 30 min for EDTA Fig. 6(a) and Co(II)-EDTA Fig. 7(a), it can be seen that EDTA is removed efficiently more than Co(II)-EDTA. This may be due to the complexed geometry of Co(II)-EDTA complexes compared to free EDTA.

It can be concluded from Fig. 7(a) that both MMPC and CSPC have low affinity for Co(II)-EDTA species. This illustrates that the removals attained after 30 min are mainly due to photodegradation. The enhancement in Co(II)-EDTA removal might be due to participation of adsorption with photodegradtion. This is due to that the metals in the LDH layer (Mg(II) and Al(III)) might introduce a defect energy level, which can enhance the valence band electrons transmission to conduction band of lower energy.

It is well known that the utilization of TiO_2 for treatment as photocatalysts has found many difficulties in its separation from aqueous solution. On the contrary, the employed materials in the present work (MMPC and CSPC) not only removed EDTA and Co(II)-EDTA effectively, but also were easily separated from the aqueous phase during the experimental work.

An overview of the overall process was proposed and depicted in Fig. 8.

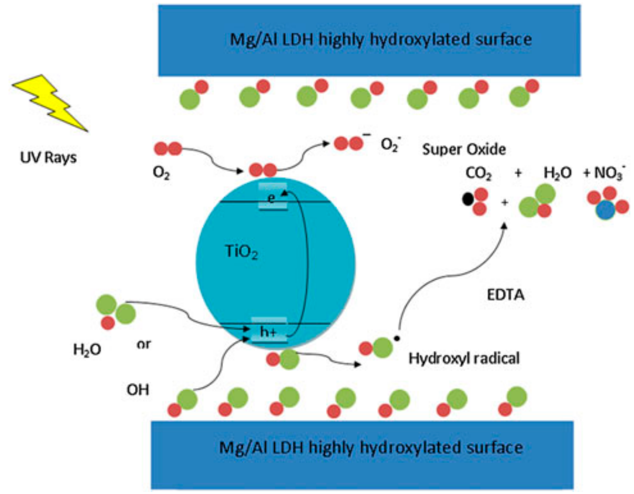

Fig. 8. A proposed schematic diagram of synchronization processes between LDH and TiO_2.

4. Conclusion

MMPC and CSPC composites were successfully prepared via co-precipitation method. The preparation method produced efficient photocatalysts, which showed an increase in the removal efficiency of EDTA and Co(II)-EDTA complexes when compared to TiO_2. The removals obtained by MMPC and CSPC are attributed to synchronization between adsorption and photodegradation. The metals of LDH layer (Mg(II) and Al (III)) introduced a defect energy level, which enhanced the valence band electrons transmission to conduction band of lower energy. The removal efficiency of EDTA reached up to 88 and 83.6% using CSPC and MMPC, respectively. Also, the removal percentage of Co-EDTA complexes is found to be 81 and 71% for CSPC and MMPC, respectively. Based on the data obtained in the present study, the employed photocatalysts have a great potential in wastewater treatment technology.

Acknowledgements

Authors kindly introduce their deep thanks to all the staff members of Nuclear Chemistry Department at EAEA for their continuous support. Many thanks are also introduced to Dr Moustafa Shawky (CMRDI) and Dr Ahmed Rashad (EPRI) for their help during the characterization of the photocatalysts.

References

[1] P.J. Majewski, Removal of organic matter in water by functionalised self-assembled monolayers on silica, Sep. Purif. Technol. 57 (2007) 283–288.

[2] E.D. Tusnelda, H.F. Fritz, Removal of selected persistent organic pollutants by heterogeneous photocatalysis in water, Catal. Today 101 (2005) 195–202.

[3] S. Lin, C. Chiou, C. Chang, R. Juang, Photocatalytic degradation of phenol on different phases of TiO_2 particles in aqueous suspensions under UV irradiation, J. Environ. Manage. 92 (2011) 3098–3104.

[4] R. Takeuchi, Y. Suwa, T. Yamagishi, Y. Yonezawa, Anaerobic transformation of chlorophenols in methanogenic sludge unexposed to chlorophenols, Chemosphere 41 (2000) 1457–1462.

[5] J. Wang, X. Wang, G. Li, P. Guo, Z. Luo, Degradation of EDTA in aqueous solution by using ozonolysis and ozonolysis combined with sonolysis, J. Hazard. Mater. 176 (2010) 333–338.

[6] K. Parida, L. Mohapatra, N. Baliarsingh, Effect of Co^{2+} substitution in the frame-work of carbonate intercalated Cu/Cr LDH on structural, electronic, optical, and photocatalytic properties, J. Phys. Chem. 116 (2012) 22417–22424.

[7] S.J. Xia, F.X. Liu, Z.M. Ni, W. Shi, J.L. Xue, P.P. Qian, Ti-based layered double hydroxides: Efficient photocatalysts for azo dyes degradation under visible light, Appl. Catal., B Environ. 144 (2014) 570–579.

[8] A. Fujishima, X. Zhang, D.A. Tryk, TiO_2 photocatalysis and related surface phenomena, Surf. Sci. Rep. 63 (2008) 515–582.

[9] A. Di Paola, E. García-López, G. Marcì, L. Palmisano, A survey of photocatalytic materials for environmental remediation, J. Hazard. Mater. 211–212 (2012) 3–29.

[10] M.N. Chong, B. Jin, C.W.K. Chow, C. Saint, Recent developments in photocatalytic water treatment technology: A review, Water Res. 44 (2010) 2997–3027.

[11] C. Hu, Y.Z. Wang, H.X. Tang, Destruction of EDTA aqueous solution by photocatalysis or direct photolysis, Chemosphere 41 (2000) 1205–1209.

[12] E.M. Seftel, M.C. Puscasu, M. Mertens, P. Cool, G. Carja, Assemblies of nanoparticles of CeO_2–ZnTi-LDHs and their derived mixed oxides as novel photocatalytic systems for phenol degradation, Appl. Catal., B Environ. 150–151 (2014) 157–166.

[13] E.M. Seftel, E. Popovici, M. Mertens, G.V. Tendeloo, P. Cool, E.F. Vansant, The influence of the cationic ratio on the incorporation of Ti^{4+} in the brucite-like sheets of layered double hydroxides, Microporous Mesoporous Mater. 111 (2008) 12–17.

[14] F. Kovanda, E. Jindová, K. Lang, P. Kubát, Z. Sedláková, Preparation of layered double hydroxides intercalated with organic anions and their application in LDH/poly(butyl methacrylate) nanocomposites, Appl. Clay Sci. 48 (2010) 260–270.

[15] M. Herrero, S. Martínez-Gallegos, F.M. Labajos, V. Rives, Layered double hydroxide/polyethylene terephthalate nanocomposites. Influence of the intercalated LDH anion and the type of polymerization heating method, J. Solid State Chem. 184 (2011) 2862–2869.

[16] J.S. Valente, F. Tzompantzi, J. Prince, Highly efficient photocatalytic elimination of phenol and chlorinated phenols by CeO_2/MgAl layered double hydroxides, Appl. Catal., B Environ. 102 (2011) 276–285.

[17] K.H. Goh, T.T. Lim, A. Banas, Z. Dong, Sorption characteristics and mechanisms of oxyanions and oxyhalides having different molecular properties on Mg/Al layered double hydroxide nanoparticles, J. Hazard. Mater. 179 (2010) 818–827.

[18] M. Gallastegi-Villa, A. Aranzabal, M. Romero-Sáez, J.A. González-Marcos, J.R. González-Velasco, Catalytic activity of regenerated catalyst after the oxidation of 1,2-dichloroethane and trichloroethylene, Chem. Eng. J. 241 (2014) 200–206.

[19] J. Zhu, H. Fan, J. Sun, S. Ai, Anion-exchange precipitation synthesis of α-Ag_2WO_4/Zn–Cr layered double hydroxides composite with enhanced visible-light-driven photocatalytic activity, Sep. Purif. Technol. 120 (2013) 134–140.

[20] H. Zhao, K.L. Nagy, Dodecyl sulfate–hydrotalcite nanocomposites for trapping chlorinated organic pollutants in water, J. Colloid Interface Sci. 274 (2004) 613–624.

[21] R. Lu, X. Xu, J. Chang, Y. Zhu, S. Xu, F. Zhang, Improvement of photocatalytic activity of TiO_2 nanoparticles on selectively reconstructed layered double hydroxide, Appl. Catal., B Environ. 111–112 (2012) 389–396.

[22] E. Dvininov, M. Ignat, P. Barvinschi, M.A. Smithers, E. Popovici, New SnO_2/MgAl-layered double hydroxide composites as photocatalysts for cationic dyes bleaching, J. Hazard. Mater. 177 (2010) 150–158.

[23] S.P. Paredes, M. Valenzuela, G. Fetter, S.O. Flores, TiO_2/MgAl layered double hydroxides mechanical mixtures as efficient photocatalysts in EDTA degradation, J. Phys. Chem. Solids 72 (2011) 914–919.

[24] T. Kameda, M. Saito, Y. Umetsu, Preparation and characterisation of Mg–Al layered double hydroxides intercalated with 2-naphthalene sulphonate and 2,6-naphthalene disulphonate, Mater. Trans. 47 (2006) 923–930.

[25] P. Pookmanee, S. Phanichphant, Titanium dioxide powder prepared by a sol-gel method, J. Ceram. Process. Res. 10 (2009) 167–170.

[26] N. Kumar, V. Dutta, Synthesis of hollow CdS micro-/nanospheres by CoSP technique and their visible light photocatalytic activities, Appl. Surf. Sci. 288 (2014) 172–179.

[27] G. Chen, S. Qian, X. Tu, X. Wei, J. Zou, L. Leng, S. Luo, Enhancement photocatalytic degradation of rhodamine B on nano Pt intercalated Zn–Ti layered double hydroxides, Appl. Surf. Sci. 293 (2014) 345–351.

[28] K.H. Goh, T.T. Lim, A. Banas, Z. Dong, Application of layered double hydroxides for removal of oxyanions: A review, Water Res. 42 (2008) 1343–1368.